Origins of the two-step relaxation and the boson peak in an alkali silicate glass studied by molecular-dynamics simulation

J. Habasaki and I. Okada
Tokyo Institute of Technology at Nagatsuta, Yokohamsa, Kanagawa 226, Japan

Y. Hiwatari
Kanazawa University, Kanazawa 920-11, Japan

A molecular-dynamics simulation of lithium metasilicate (Li_2SiO_3) has been performed. A clear two-step relaxation was observed at 700 K in a density correlation function (self-part) for Li ions following an exponential decay by vibrational motion. Oscillation is found in the second (β relaxation) region of the function, which is attributed to the so-called "boson peak." The oscillation is clearer for O and Si than for Li. The slowest relaxation (α relaxation) can be well fitted to a stretched exponential form, and an origin of this type of decay is confirmed to be a waiting time distribution of jump motions. Both the β relaxation and the boson peak are found to be due to correlated motion.

PACS number(s): 61.20.−p, 63.50.+x

I. INTRODUCTION

During the past years, many studies, both experimental and theoretical, on slow dynamics near the glass transition temperature have been performed mainly for the so-called "fragile" glasses [1], which have no directional bonds and show an abrupt increase in viscosity upon supercooling. On the other hand, systems having covalent or hydrogen-bonded frameworks are often classified as "strong" glass systems. Experimentally, the fast β and slower α relaxations are known to exist near the glass transition region in several fragile materials [2]. Recently, such a two-step relaxation has also been reported for a strong network forming glass B_2O_3 [3]. This suggests that the two-step relaxation is a more general phenomenon than had been previously expected. The main purpose of the present work is to study the slow dynamics and related properties of lithium metasilicate (Li_2SiO_3) glass by means of molecular dynamics (MD) simulation. A silica (SiO_2) glass system, which is a typical strong system, is known to change to a more fragile one by addition of alkali oxide, since the framework structure is broken by such doped alkali-metal ions. Therefore, detailed analyses of such a system may be helpful for a better understanding of the relationships between the relaxation process and the fragility.

II. METHOD

The MD calculation was performed in the same way as in our previous studies [4–8]. The periodic cube contained 144 Li, 72 Si, and 216 oxygen atoms. A Gilbert-Ida-type potential function plus an r^{-6} term was used, i.e.,

$$\phi_{ij} = z_i z_j e^2 / r + f_0(b_i + b_j)$$
$$\times \exp(a_i + a_j - r)/(b_i + b_j) - c_i c_j / r^6, \qquad (1)$$

where z is the effective charge number; e is the elementary charge; a, b, and c are the parameters characteristic of each atom; and f_0 is a normalization constant (4.184 $kJ\,Å^{-1}\,mol^{-1}$). The potential parameters used in this work were previously derived from an *ab initio* molecular orbital calculation [4]. The system was equilibrated at 4000 K for more than 10 000 time steps, starting from a random configuration, and then the system was cooled down to lower temperatures. Simulation runs were carried out at 3000, 2000, 1673, 1173, 973, and 700 K. The step time was 1 fs from 4000 to 2000 K and 4 fs from 1673 K to 700 K. The velocities of all particles were initially set to zero at each temperature and several thousand steps were carried out at constant temperature and pressure (0.1 MPa). Then the sizes of the periodic cube were fixed to the equilibrated or quasiequilibrated volumes. In the present work, analyses were made for the simulation data at 1673 K and 700 K. The MD run was carried out for 8000 steps at 1673 K and 200 000 steps at 700 K at a constant energy condition.

III. CHARACTERISTICS OF THE STRUCTURE OF LITHIUM METASILICATE

The result of the detailed structural analysis of the Li_2SiO_3 system was reported in our previous work [5]. The system consists of branched-chain structures composed of SiO_4 tetrahedral units and Li^+ ions surrounded by oxygen atoms. It is worth noting that the system is regarded as fragile for Li^+ ions and strong for Si and O atoms of the chain structure as will be mentioned later,

although the fragility was originally defined for the overall system [1]. However, to discuss the remarkable differences in dynamical behavior of the three kinds of the atoms, it is useful to consider not only the fragility of the system, but also the fragility of the atoms. The glass transition temperature T_g of this system obtained by the volume-temperature relation is 830 ± 50 K, which is comparable with the experimental value 687 K [9]. Theoretical and experimental determinations of T_g do not necessarily agree with each other [10,11]. The inflection point of the temperature-volume curve denotes nothing but the temperature at which the relaxation time for volume fluctuations becomes comparable with the simulation time [12]. However, the origin of such inflection is not purely kinetic, and a saturation of the packing of the oxygen atoms in the first coordination shell has also been found to occur at this point [6–8].

IV. RESULTS AND DISCUSSION

A. Mean squared displacement

Mean squared displacements of the Li, O, and Si atoms at 700 K are shown on logarithmic scales in Fig. 1. Similar results were obtained in a previous study with a set of empirical potentials [5]. The statistics of the present calculations is better than those of the previous ones. Except for the early time region, nonlinear time-dependent behavior is observed. This behavior is similar to that of a soft core system [13]. The value for Li ion increases between 1 and 10 ps and those for Si and O slightly increase between 1 and 70 ps. An increase in the curve is observed for each atom in a larger t region. Colmenero et al. [14] have observed an increase in the curve for the mean squared displacement obtained from a normalized intermediate scattering function $I_0(\mathbf{Q}, t)$ of a fragile glass-forming polymer by neutron scattering experiments. They attributed it to an artifact due to the cutoff in the deconvolution process. This argument does not hold, however, for the present case because the mean
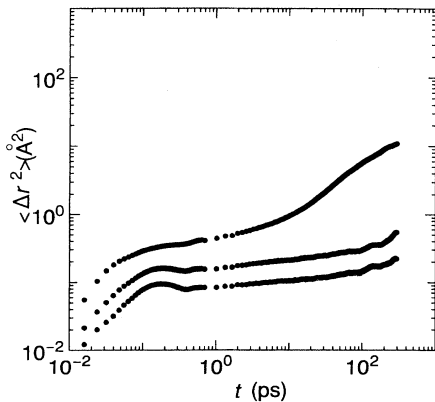
squared displacements in Fig. 1 are directly obtained from the motion of the atoms in real space. The part of the curve with increasing mean squared displacement corresponds to the α-relaxation region discussed below.

B. Density correlation function (self-part)

The density correlation function (self-part) $F_s(\mathbf{k}, t)$ was calculated for a wide range of time, where $F_s(\mathbf{k}, t)$ is
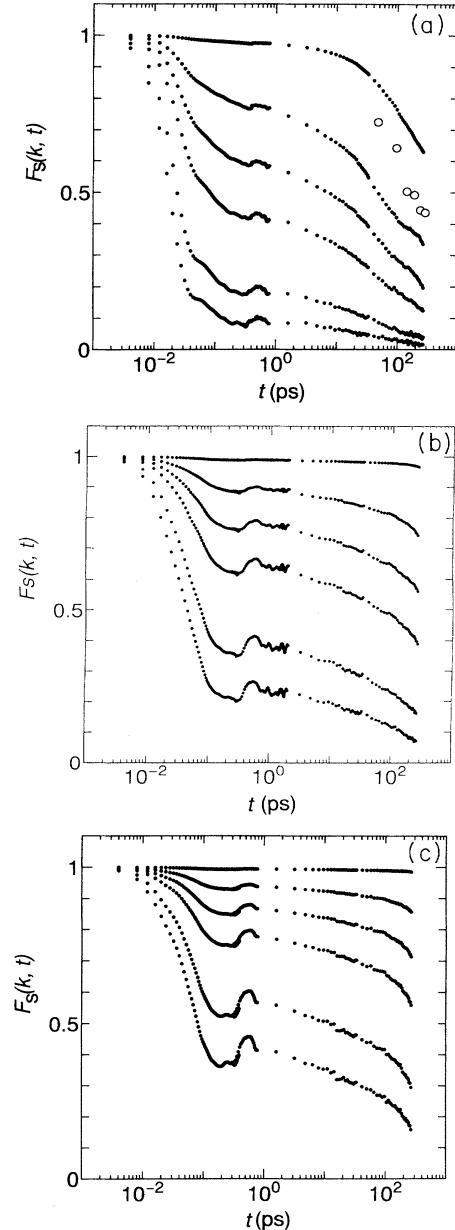

FIG. 2. Density correlation function (self-part) of (a) Li, (b) O, and (c) Si at 700 K. The curves from top to bottom are for wave numbers $k = 2\pi/n'$ ($n' = 10, 3, 2, 1.5, 1, 0.8$) in units of Å^{-1}. The circles in (a) are obtained from the area under the first peak of the van Hove function (self-part) $4\pi r^2 Gs(r, t)$ for Li.

FIG. 1. Mean square displacements of the atoms at 700 K on a log-log scale. The curves from top to bottom are for Li, O, and Si, respectively.
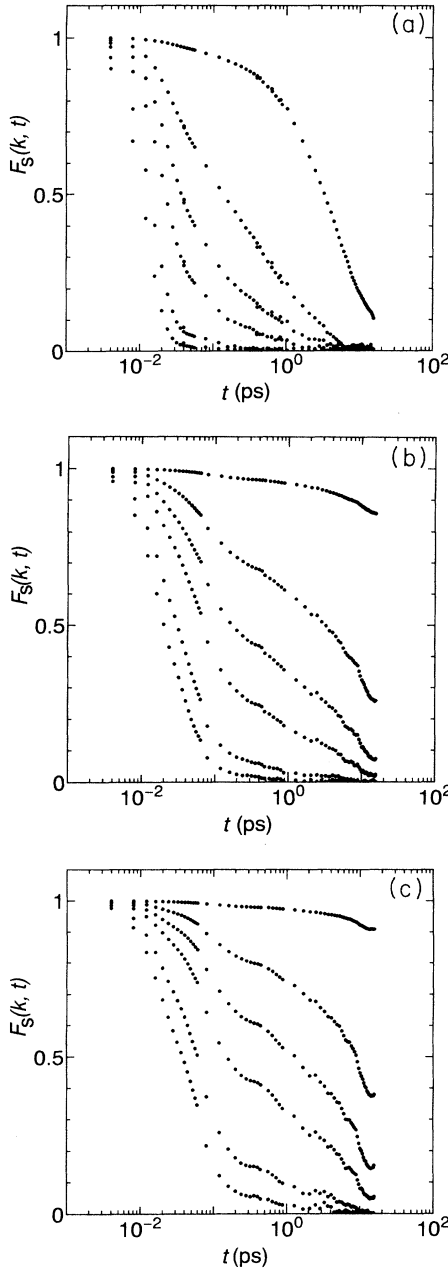
FIG. 3. Density correlation function (self-part) of (a) Li, (b) O, and (c) Si at 1673 K. The curves from top to bottom are for wave numbers $k = 2\pi/n'$ $(n' = 10, 3, 2, 1.5, 1, 0.8)$ in units of Å^{-1}.

defined as

$$F_s(\mathbf{k}, t) = \left\langle \sum_{j=1}^{N_{\alpha'}} \exp\{i\mathbf{k} \cdot d\mathbf{r}_j^{\alpha'}(t)\} \right\rangle \Big/ N_{\alpha'}, \qquad (2)$$

α' denotes the species indices, and $\langle \rangle$ denotes an initial time average. For Li, O, and Si at 700 K, a clear two-step slow relaxation is observed following an exponential decay by vibrational motion (Fig. 2). In the present work, the first slow-relaxation process is termed the "β relax-

ation" and the second slow-relaxation process is termed the "α relaxation." In Fig. 3 the respective data for Li, O, and Si at 1673 K are shown. The function decays exponentially at less than 0.1 ps for each species. The boundary between α and β relaxations is not clear. The curve can be fitted to an exponential function after 1 ps.

C. Fast-relaxation process

We have fitted the fast (~ 0.1 ps) decay of $F_s(\mathbf{k}, t)$ by a Debye-like expression

$$F_s(\mathbf{k}, t) = \exp[-(t/\tau)]. \qquad (3)$$

The parameters of best fit at 700 K and 1673 K are listed in Tables I and II, respectively. The relaxation time of the fast Debye region is expressed by $\tau \propto \mathbf{k}^{-2}$ at both temperatures.

D. β-relaxation process

An oscillating process was found in the second region (0.1–10 ps) of $F_s(\mathbf{k}, t)$ for Li, O, and Si at 700 K. The oscillation is deeper for O and Si than for Li. The decays for O and Si during this period are smaller than for Li. Low-frequency vibrational excitation is known to contribute

TABLE I. Fitted parameters at 700 K for the initial decay in the form $\exp(-t/\tau_k)$. An asterisk denotes the best fitted lines for the k dependence of τ_k.

$\mathbf{k}$ (Å^{-1})	τ_k (ps)
Li	
$2\pi/10$	3.39
$2\pi/3$	0.31
$2\pi/2$	0.14
$2\pi/1.5$	0.078
$2\pi/1$	0.037
$2\pi/0.8$	0.025

$\ln \tau_k = 0.124 - 1.96 \ln \mathbf{k}^*$

$\mathbf{k}$ (Å^{-1})	τ_k (ps)
Si	
$2\pi/10$	18.4
$2\pi/3$	1.65
$2\pi/2$	0.73
$2\pi/1.5$	0.41
$2\pi/1$	0.18
$2\pi/0.8$	0.12

$\ln \tau_k = 1.98 - 2.00 \ln \mathbf{k}^*$

$\mathbf{k}$ (Å^{-1})	τ_k (ps)
O	
$2\pi/10$	9.81
$2\pi/3$	0.88
$2\pi/2$	0.40
$2\pi/1.5$	0.22
$2\pi/1$	0.10
$2\pi/0.8$	0.065

$\ln \tau_k = 1.36 - 1.99 \ln \mathbf{k}^*$

TABLE II. Fitted parameters at 1673 K for the initial decay in the form $\exp(-t/\tau_k)$. An asterisk denotes the best fitted lines for the k dependence of τ_k.

k (Å^{-1})	τ_k (ps)
Li	
$2\pi/10$	1.20
$2\pi/3$	0.11
$2\pi/2$	0.049
$2\pi/1.5$	0.028
$2\pi/1$	0.013
$2\pi/0.8$	0.0087

$\ln \tau_k = -0.76 - 1.96 \ln k^*$

Si	
$2\pi/10$	83.75
$2\pi/3$	0.755
$2\pi/2$	0.336
$2\pi/1.5$	0.189
$2\pi/1$	0.084
$2\pi/0.8$	0.054

$\ln \tau_k = 1.20 - 2.00 \ln k^*$

O	
$2\pi/10$	4.29
$2\pi/3$	0.44
$2\pi/2$	0.18
$2\pi/1.5$	0.099
$2\pi/1$	0.045
$2\pi/0.8$	0.030

$\ln \tau_k = 0.62 - 2.03 \ln k^*$

to the dynamics of some glasses near the glass transition temperature. For example, at low temperatures a broad inelastic hump was found around 2.3 meV (1 eV=96.5 kJ mol^{-1}) in the incoherent scattering function $S(Q,\omega)$ of polyisobutylene [15]. The mode coupling theory [10] was not conceived to describe such inelastic low-frequency excitation. In low-frequency Raman spectra, these kinds of excitations are well known as the so-called "boson peak" [16], which has not been found in very fragile systems. The differences of the depth of oscillation observed in the present work, which are consistent with this experimental observation, are understood in terms of the fragility of each species. Thus the motions of atoms for Li_2SiO_3 in this time region were examined in detail. In Fig. 4, x-y projection of the motion of the particles during 1.0 ps within a cube $(10 \times 10 \times 10 \text{ Å}^3)$ is shown, where the thermal oscillation is removed by taking an average of each 0.2-ps run. The position of the atoms at $t = 0$ and $t = 0.2$ ps are marked. The neighboring Si-O pairs (cut-off length is set to be 2.0 Å) are connected to clarify the chain structure. As shown in the Fig. 4, some atoms move collectively at the same time. (For example, see the motion of atoms within circles.) The collective motion is similar to that observed in the soft core system [17]. Correlation of the motion of atoms is not restricted to the connected structure (SiO_4 chain) but includes those of
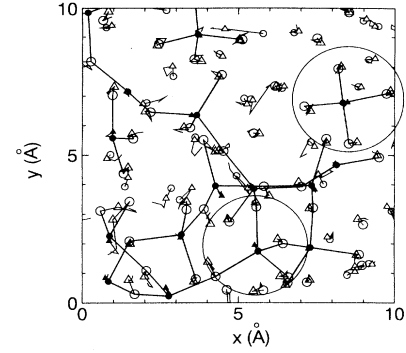

FIG. 4. x-y projections of the motion of the particles during 1.0 ps within a cube $(10 \times 10 \times 10 \text{ Å}^3)$. Positions at $t = 0$ of Li (○), Si (●), and O (◯) are marked. The triangles are for the positions at $t = 0.2$ ps (positions were averaged for each 0.2 ps).

neighboring Li. Buchenau et al. [18] studied the vibrational excitation in vitreous silica by inelastic scattering of cold neutrons and identified the low-frequency mode as a coupled rotation of SiO_4 tetrahedra. However, the correlated motion observed in the present work is not a simple coupled rotation. A detailed analysis for this kind of motion will be given elsewhere. The distinct part of the van Hove function is defined by

$$G_d^{\alpha'\beta'}(\mathbf{r},t) = (1/N_{\alpha'}) \sum_{i=1}^{N_{\alpha'}} \sum_{j=1}^{N_{\beta'}} \langle \delta(\mathbf{r} - \mathbf{r}_i^{\alpha'}(0) + \mathbf{r}_j^{\beta'}(t)) \rangle,$$

(4)

where $\mathbf{r}_i^{\alpha'}$ denotes the position of particle i of species α' at time t and the self-term $i = j$ is to be left out if $\alpha' = \beta'$. $N^{\alpha'}$ and $N^{\beta'}$ are the number of particles of species α' and β', respectively. In Fig. 5(a) the van Hove function (distinct part) for the O-O pair is shown, where the time region corresponds to the β-relaxation region (less than 1.0 ps). It is noteworthy that the peak height is not necessarily sequenced with the elapse of time, that is, the oscillation of the peak height occurs during 0–1.0 ps. Peak positions are unchanged during this period but oscillation of the peak width occurs. Similar behavior is observed for the Si-O, O-Si, and Si-Si pairs, which corresponds to the oscillation in the density correlation function. In Fig. 5(b) the function for the Li-O pair is shown. The curves overlap and the oscillation is unclear. During this period, the peak position shifts toward higher r. Similar behavior is observed for the Li-Li and O-Li pairs. The shift can be attributed to the β relaxation. The observed characteristics in the function are due to the correlated motion as shown in Fig. 4. Thus the β relaxation occurs in the same region with the oscillating motions both in space and time. The process seems to have the same microscopic origin as the oscillating motions earlier suggested by Sokolov et al. [19]. They also suggested that in a strong structure, such as chains, an oscillating process is dominant, while in a fragile struc-
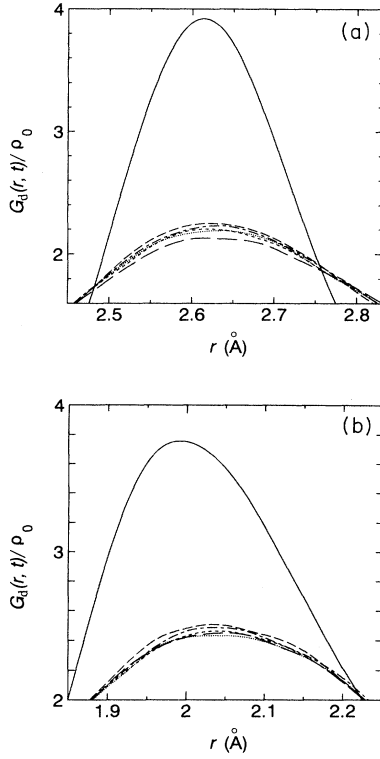
FIG. 5. The van Hove function (distinct part) for (a) the O-O pair and (b) the Li-O pair in the β-relaxation region at 700 K (—, $t = 0$; — —, $t = 0.2$; - - -, $t = 0.4$; - - -, $t = 0.6$; - - - -, $t = 0.8$; $\cdots$, $t = 1.0$).

TABLE III. Fitted parameters at 700 K for the α decay in the form $A\exp[-(t/\tau_k)^\beta]$. An asterisk denotes the best fitted lines for the **k** dependence of τ_k, where the values for the smallest **k** are omitted.

k (Å^{-1})	A	β	τ_k (ps)
	Li		
$2\pi/10$	1.00	0.60	899
$2\pi/3$	0.94	0.32	229
$2\pi/2$	0.68	0.38	162
$2\pi/1.5$	0.52	0.35	96.8
$2\pi/1$	0.24	0.37	47.5
$2\pi/0.8$	0.12	0.37	40.3

$\ln \tau_k = 6.56 - 1.41 \ln k^*$

k	A	β	τ_k
	Si		
$2\pi/10$	0.99	0.82	109×10^3
$2\pi/3$	0.93	0.65	13.7×10^3
$2\pi/2$	0.86	0.63	4.60×10^3
$2\pi/1.5$	0.76	0.60	2.24×10^3
$2\pi/1$	0.56	0.53	784
$2\pi/0.8$	0.42	0.50	385

$\ln \tau_k = 11.52 - 2.67 \ln k^*$

k	A	β	τ_k
	O		
$2\pi/10$	0.99	0.93	20.6×10^3
$2\pi/3$	0.88	0.58	6.50×10^3
$2\pi/2$	0.78	0.44	3.71×10^3
$2\pi/1.5$	0.66	0.43	1.40×10^3
$2\pi/1$	0.41	0.42	341
$2\pi/0.8$	0.26	0.46	169

$\ln \tau_k = 11.19 - 2.88 \ln k^*$

ture the relaxation process is dominant. In other words, the species forming the network structure tends to return to its original position after correlated motion.

E. α-relaxation process

An α-relaxation process is commonly expressed by a Williams-Watts-type function [20]

$$F_s(\mathbf{k}, t) = A\exp[-(t/\tau)^\beta],   (5)$$

where A, β, and τ are the adjustable parameters. When β is less than unity, the system is accompanied by slow relaxations, since the time necessary for the relaxation function to become $1/e$ times strongly increases with the elapse of time. The relaxation is of a non-Debye type in contrast to the Debye-type decay in Eq. (3). We have fitted the slow decay of $F_s(\mathbf{k}, t)$ by Eq. (5), with the parameters of best fit for Eq. (5) at 700 K being listed in Table III. The fitted parameters expressed by a simple exponential decay after 1 ps at 1673 K are given in Table IV. In previous work, the self-part of the van Hove function $4\pi r^2 G_s(\mathbf{r}, t)$ of the Li ion for long time simulation was shown to have a second peak due to the jump motions [6–8], where the function is defined as

TABLE IV. Fitted parameters at 1673 K for the region $t \geq 1.0$ ps in the form $A\exp(-t/\tau_k)$. An asterisk denotes the best fitted lines for the **k** dependence of τ_k.

k (Å^{-1})	A	τ_k (ps)	t (ps)
	Li		
$2\pi/10$	0.90	6.21	
$2\pi/3$	0.37	1.96	
$2\pi/2$	0.16	1.80	
$2\pi/1.5$	0.073	1.19	

$\ln \tau_k = 1.40 - 0.84 \ln k^*$

k	A	τ_k	t
	Si		
$2\pi/10$	0.98		190.0
$2\pi/3$	0.78		19.4
$2\pi/2$	0.57		10.5
$2\pi/1.5$	0.38		6.94

$\ln \tau_k = 4.38 - 1.77 \ln k^*$

k	A	τ_k	t
	O		
$2\pi/10$	0.96		131.6
$2\pi/3$	0.95		15.88
$2\pi/2$	0.39		8.47
$2\pi/1.5$	0.20		6.17

$\ln \tau_k = 4.08 - 1.65 \ln k^*$

$$G_s^{\alpha'}(\mathbf{r},t) = (1/N_{\alpha'}) \sum_{i=1}^{N_{\alpha'}} \langle \delta(\mathbf{r}_i^{\alpha'}(t) - \mathbf{r}_i^{\alpha'}(0) - \mathbf{r}) \rangle. \quad (6)$$

The number of ions in the original site was calculated from $\int_0^{r_c} 4\pi r^2 G_s(r,t)dr$, where r_c is chosen to be half of the distance of $g_{\max}^{\mathrm{Li\text{-}Li}}(\mathbf{r})$. The decrease of the area can be well represented by a stretched-exponential form and the fitted parameters for Li are $A=0.923$, $\beta=0.583$, and $\tau_j =448$ ps. This result clearly shows that the origin of the stretched exponential form is due to the distribution of the jump rate τ_j. Comparison of these values with those in Table III reveals that the origin of the α relaxation of the Li ion observed in $F_s(k,t)$ is also the jump motion. In the trapping diffusion model [11], the waiting time distribution of the jump is regarded as the origin of stretched-exponential-type dynamics. The results in this work are consistent with this model. The jump rate is related to the local structure around the jump site. We have already shown that the lifetime of the structure composed of O atoms around Li differs according to the geometrical degree of freedom of the polyhedra [6–8]. Jump motion of some oxygen atoms has already been analyzed in our previous study [6], where the rotational motion of SiO$_4$ units contributes to the mean squared displacements of O. The frequency of jumps of O is smaller than those of Li ions.

Figures 6(a) and 6(b) show $G_d(r,t)$'s for O-O and Si-Si, respectively, with longer time scale than in Fig. 5. For
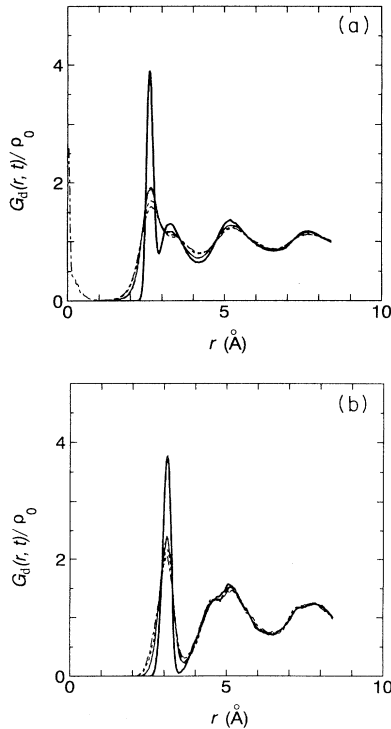

FIG. 6. The van Hove function (distinct part) for (a) the O-O pair and (b) the Si-Si pair. The curves from top to bottom in the original first peak are for $t = 0,48,96,192,336$ ps.
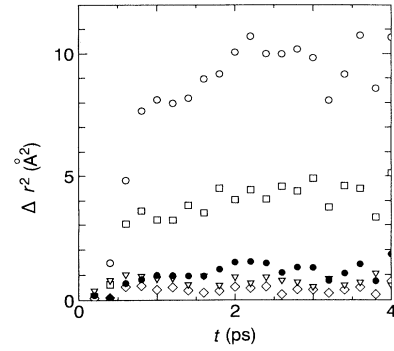

FIG. 7. Square displacement of Si ($\bullet$) is plotted versus time with those of the surrounding O atoms ($\circ, \diamond, \nabla, \square$).

the O-O pair, the small peak at $r = 0$ due to a jump of O to the site previously occupied by the other O is found. Meanwhile, for Si-Si pairs, no peak is found at $r = 0$. The G_d functions reveal that site-site jumping by Si did not occur during the simulation time, that is, 336 ps. The squared displacement of an Si atom is plotted versus time with those of the surrounding O atoms in Fig. 7, where the thermal oscillation is removed by taking an average for each 0.2 ps. The figure demonstrates the small jump motion of the Si atom, which is clearly correlated with the motion of neighboring O atoms.

The dependence of A, β, and τ values in Eq. (5) on wave number $\mathbf{k}$ at 700 K is examined. The value A in Table III can be well represented by a linear function of $\mathbf{k}$. The order of magnitude of A for each $\mathbf{k}$ is Si>O>Li. A larger A value means that the structural change during the initial and the β process is smaller. The smaller Li ion has the largest mobility and Si, which is located at the center of the SiO$_4$ tetrahedron, has the smallest mobility in the early time region. The larger $\mathbf{k}$ dependence of A for Li is also attributable to the highest mobility of the small ion in the large $\mathbf{k}$ area in this time region. The value of β is found to be less than 1 at 700 K for all the species, with minima at about 2 Å^{-1} for Li and at 4 Å^{-1} for O. The value for Si seems not to have a minimum in the $\mathbf{k}$ range investigated. This trend may be interpreted if the β has a minimum value at $\mathbf{k}$ corresponding to the inverse of the jump distance of each species. It should be taken into account, however, that the fitted values for the small $\mathbf{k}$ values involve fairly large errors especially for Si and O because of the slow-relaxation time compared with the simulation time. The order of β is Si>O>Li for each $\mathbf{k}$ value, as expected from the fragility of the species, and as the system becomes more fragile, β seems to decrease. This result is consistent with the suggestions by several authors [21,22], although the non-Arrhenius behavior is not necessarily equal to the nonexponential one as will be discussed later. As the origin of the non-exponential is a distribution of jump rate, the lower β value should be due to larger difference of local environments of the jump sites.

The relaxation time τ_k in Table III can be well represented by the linear function of $\mathbf{k}$ on a log-log scale at

700 K, with a larger slope for Si and O than for Li. In the Rouse model [23], τ_k is known to be proportional to k^{-n} with $n = 4$. The larger slope of **k** on the τ_k for each Si and O corresponds to the large connectivity. Namely, long-range motion is restricted due to the chain structure. On the other hand, the slope for Li is less than the value expected for the Debye-type relaxation ($n = 2$). The results suggest that the **k** dependence of τ_k for Li is affected by features of the jump motion, such as a jump path. Therefore, the τ has a distribution related to the fractal dimension of space in the system. Colmenero *et al.* [24] suggested that the $I(\mathbf{Q}, t)$ is given by the exponent $n\beta$ and found that the product is close to 2 for three polymers. The constant product obtained by them may be rather fortuitous. In the present work, the fragile Li ion has lower values of both n and β at 700 K than Si and O have. In each species, n is larger and β is smaller at 700 K than at 1673 K, as shown in Tables III and IV. Elmroth *et al.* [25] have shown that there is no simple correlation of non-Arrhenius with nonexponential behavior. This may be also explained if both n and β are taken into account. In other words, the difference in fragility contains the effect of fractal dimensions in both time and space.

V. CONCLUSION

A molecular dynamics simulation of lithium metasilicate glass (Li_2SiO_3) has been performed. A clear two-step relaxation was observed at 700 K in a density correlation function (self-part) for Li ion following an exponential decay by vibrational motion. Oscillation is found in the second (β relaxation) region of the function. The oscillation is clearer for O and Si than for Li. Namely, in a strong structure an oscillating process is dominant, while in a fragile structure, the relaxation process is dominant. Both the β relaxation and the oscillation are found to be due to the correlated motion in the same time and space regions. The slowest relaxation (α relaxation) can be well fitted to a stretched-exponential form $F_s(\mathbf{k}, t) = A\exp[-(t/\tau)^\beta]$. The small value of β (<1) comes from the the waiting time distribution of the jump motions. The relaxation time τ_k behaves as $\mathbf{k}^{-n}$ with a larger slope for Si and O than for Li. The value n is related to the fractal dimension of space in the system. Fractal dimensions of both time and space determine the relaxation behavior of the system near the glass transition temperature.

ACKNOWLEDGMENTS

[1] C. A. Angell, J. Phys. Chem. Solids **49**, 863 (1988); C. A. Angell, L. Monnerie, and L. M. Torell, in *Structure, Relaxation, and Physical Aging of Glassy Polymers*, edited by R. J. Roe and J. M. O'Relly, MRS Symposia Proceedings No. 215 (Materials Research Society, Pittsburgh, 1991).

[2] F. Mezei, W. Knaak, and B. Faragol, Phys. Rev. Lett. **58**, 571 (1987); F. Mezei, J. Non-Cryst. Solids **131-133**, 317 (1991); W. Knaak, F. Mezei, and B. Farago, Europhys. Lett. **7**, 529 (1988).

[3] D. Sidebottom, R. Bergman, L. Borjesson, and L. M. Torell, Phys. Rev. Lett. **71**, 2260 (1993).

[4] J. Habasaki and I. Okada, Mol. Simul. **9**, 319 (1992).

[5] J. Habasaki and I. Okada, Mol. Simul. **8**, 179 (1992).

[6] J. Habasaki, I. Okada, and Y. Hiwatari, Mol. Simul. **9**, 49 (1992).

[7] J. Habasaki, Mol. Phys. **70**, 513 (1990).

[8] J. Habasaki, I. Okada, and Y. Hiwatari, in *Molecular Dynamics Simulations*, edited by F. Yonezawa, Springer Series in Solid State Science Vol. 103 (Springer, New York, 1992), p. 98.

[9] M. Tatsumisago, T. Minami, and M. Tanaka, Yogyo-Kyokai-Shi **93**, 581 (1985).

[10] W. Götze, in *Liquids, Freezing and Glass Transition*, edited by J. P. Hansen, D. Levesque, and J. Zinn-Justin (North-Holland, Amsterdam, 1991), p. 287.

[11] Y. Hiwatari, H. Miyagawa, and T. Odagaki, Solid State Ionics **47**, 179 (1991).

[12] C. A. Angell, J. H. R. Clarke, and L. V. Woodcock, Adv. Chem. Phys. **48**, 397 (1981); G. H. Fredrickson, Annu. Rev. Phys. Chem. **39**, 149 (1988).

[13] H. Miyagawa, Y. Hiwatari, B. Bernu, and J. P. Hansen, J. Chem. Phys. **88**, 3879 (1988).

[14] J. Colmenero, A. Arbe, and A. Alegria, Phys. Rev. Lett. **71**, 2603 (1993).

[15] B. Frick and D. Richter, Phys. Rev. B **47**, 14 795 (1993).

[16] V. Z. Gochiyaev, V. K. Malinovsky, V. N. Novikov, and A. P. Sokolov, Philos. Mag. B **63**, 777 (1991); M. Kruger, M. Soltwisch, I. Petscherizin, and D. Quitmann, J. Chem. Phys. **96**, 7352 (1992).

[17] T. Muranaka and Y. Hiwatari, Phys. Rev. E **51**, 2735 (1995).

[18] U. Buchenau, N. Nucker, and A. J. Dianoux, Phys. Rev. Lett. **53**, 2316 (1984).

[19] A. P. Sokolov, E. Rossler, K. Kisliuk, and D. Quitmann, Phys. Rev. Lett. **71**, 2062 (1993).

[20] G. Williams and D. C. Watts, Trans. Faraday Soc. **66**, 80 (1970).

[21] T. A. Vilgis, Phys. Rev. B **47**, 2882 (1993).

[22] P. J. Plazek and K. L. Ngai, Macromolecules **29**, 1222 (1991).

[23] P. E. Rouse, J. Chem. Phys. **21**, 1273 (1953).

[24] J. Colmenero, A. Alegria, A. Arbe, and B. Frick, Phys. Rev. Lett. **69**, 478 (1992).

[25] M. Elmroth, L. Borjesson, and L. M. Torell, in *Static and Dynamic Properties of Liquids*, Springer Proceedings in Physics Vol. 40 (Springer, Berlin, 1989), p. 118.